

A Multifunctional Microstructure for Microscope Calibration and Nanoparticle Characterization

K.-T. Liao,^a C. R. Copeland,^b J. H. Myung,^a D. Kozak,^a S. M. Stavis^{b,*}

^a*United States Food and Drug Administration, Silver Spring, MD 20993*

^b*National Institute of Standards and Technology, Gaithersburg, MD 20899*

**sstavis@nist.gov*

Recent studies¹ have introduced the utility of a simple microstructure – a slit – to confine colloidal nanoparticles for light scattering, diffusion tracking, and hydrodynamic sizing by the Stokes–Einstein equation. In contrast to tracking nanoparticles in free solution, where they rapidly diffuse in and out of focus of a widefield optical microscope, a microfluidic slit confines nanoparticles in quasi-free solution to near-best focus. This prolongs the tracking of Brownian motion and improves the statistics of mean-squared-displacement analysis as a sizing method. Although the potential precision of this method is impressive, errors in diameter of up to 15 % have occurred¹ due to a combination of experimental limitations, including imperfect control of slit depth and incomplete calibration of the microscope system. Improving accuracy is necessary to apply the method to critical assays such as quality control of particle-based therapeutics for cancer.

In this study, we integrate micropillar arrays into microfluidic slits to form a multifunctional microstructure that improves accuracy in two ways. First, the pillar height sets the slit depth, which slows diffusion in quasi-free solution and requires a hydrodynamic correction factor. Second, the pillar array builds in an accurate and precise value of pitch that enables correction of position errors due to distortion and astigmatism of the imaging field.² Together, these yield a microscopic focal volume that is under control and that has traceable dimensions.

We pattern the microstructure in silica by photolithography and reactive ion etching. Scanning electron microscopy shows nearly vertical sidewalls of the micropillars and a low roughness of the etched surface (Fig. 1a, b). Atomic force microscopy gives its root-mean-square roughness as approximately 1 nm, which is important to minimize background noise from light scattering under darkfield illumination (Fig. 2a). We form the slit by bonding the microstructure to a silica coverslip. After filling with a fluorescent solution, fluorescence microscopy shows a nearly uniform intensity between the pillars (Fig. 2b, c), demonstrating the first function of depth control. The reference value of the array pitch then allows correction of position errors from distortion and astigmatism (Fig. 3), demonstrating the second function of microscope calibration. Leveraging these two functions, we can record long trajectories of test nanoparticles (Fig. 4a) and liposomal particles containing the cancer therapeutic doxorubicin (Fig. 4b), and accurately track the diffusing particles across the imaging field (Fig 4c, d).

¹Haiden C, *et al.* Langmuir 30: 9607–9615, 2014, Appl. Phys. Lett. 108: 094101, 2016.

²Copeland CR, *et al.* Light: Science & Applications 7: 31, 2018.

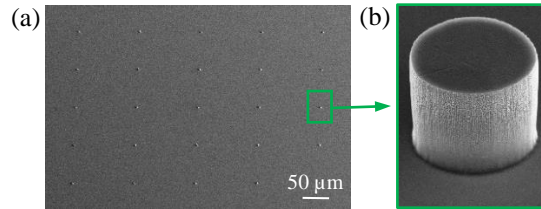


Fig. 1. (a, b) Scanning electron micrographs showing (a) a micropillar array across a slit etched to a depth of approximately $2.9\ \mu\text{m}$ and (b) a representative micropillar with nearly vertical sidewalls with respect to the etched surface. We tune the etch power to reduce redeposition of the chromium etch mask, achieving a root-mean-square surface roughness of approximately $1\ \text{nm}$, as we quantify by atomic force microscopy.

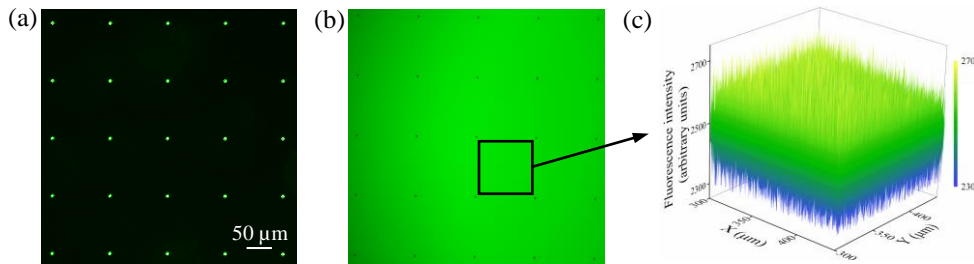


Fig. 2. (a) Darkfield optical micrograph (false color) showing a micropillar array before bonding and filling. The smooth etched surface results in low intensity of background light scattering under darkfield illumination. (b) Fluorescence optical micrograph (false color) showing the slit after bonding and filling with an aqueous solution with fluorescent molecules. (c) Plot showing nearly uniform intensity after background subtraction and flatfield correction, confirming control of slit depth.

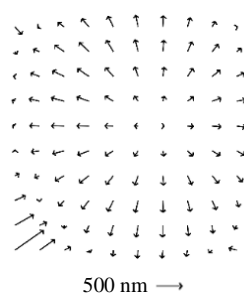


Fig. 3. Plot showing a representative correction of position errors across the imaging field, using the array pitch as a reference value. The plot pitch is $63\ \mu\text{m}$ and is not to scale with the arrow lengths. In addition to the field dependence of position errors from distortion and astigmatism, the mean value of image pixel size is less than the nominal value by approximately $3.3\ \%$. This significant deviation is consistent with our previous study of a similar microscope system using aperture arrays as independent reference materials.²

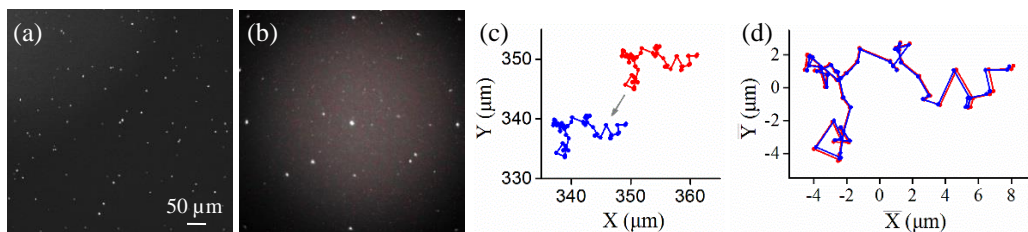


Fig. 4. (a, b) Darkfield optical micrographs showing (a) polymeric nanoparticles for test and (b) liposomal particles containing the cancer therapeutic doxorubicin for analysis. (c, d) Plots showing the trajectory of a single liposomal particle from (b) after reducing the data density by a factor of 20 for clarity, (c) before (red) and after (blue) correcting positions, and (d) after registering mean positions to clearly show the effect of variable magnification. Without this correction, position errors distort particle trajectories and field dimensions, biasing analyses of diffusion coefficient for particle sizing.